Electronic Supplementary Material (ESI) for Journal of Materials Chemistry A.

Supplementary Information for

Solvent-Free Preparation of Imine Vitrimers: Leveraging Benzoxazine Crosslinking for Melt Processability and Tunable Mechanical Performance

Levi J. Hamernik[a], William Guzman[a], & Jeffrey S. Wiggins[a*]

[a] School of Polymer Science and Engineering, University of Southern Mississippi, 118 College Drive, Hattiesburg, MS 39406, USA.

*Corresponding Author: Jeffrey.wiggins@usm.edu

Contents

.

Synthesis of Imine Benzoxazine (iBOX) Monomers:

Synthesis of D400 linked imine benzoxazine (D400-iBOX)

HBA-BA (20.33 g, 80 mmol) was added to a 100 mL one-neck round bottom flask and heated to 100 °C. Upon melting of the HBA-BA BOX monomer, Jeffamine D400 (20.31 g, 44 mmol) was added dropwise under vigorous stirring and left to react for 1 h. The reaction was then poured into an aluminum weigh pan and was transferred to a preheated vacuum oven. The material was allowed to react and degas for an additional hour at 120 °C under vacuum. The material was removed and cooled to room temperature to yield D400-iBOX as a pale yellow, viscous liquid (quantitative yield, T_g = -16.80 °C). ^{1}H NMR (600 MHz, DMSO-*d*6) δ 8.18 – 8.12 (m, 2H, C*H*=N), 7.47 (d, *J* = 8.4 Hz, 2H, C*H* aromatic), 7.37 – 7.30 (m, 4H, C*H* aromatic), 7.34 – 7.32 (m, 4H, C*H* aromatic), 7.30 – 7.24 (m, 2H, C*H* aromatic), 6.80 (d, *J* = 8.2 Hz, 2H, C*H* aromatic), 4.89 (s, 4H, O-CH_2-N), 3.92 (s, 4H Ar-CH_2-N), 3.83 (s, 4H Ar-CH_2-N), 3.46 (m, 15H, O- CH_2-CH), 3.38 – 3.19 (m, 5H, CH_3- C*H*-N), 1.10– 0.89 (m, 32H, CH_3- CH).

Synthesis of BAEE linked imine benzoxazine (BAEE-iBOX)

HBA-BA (35.52 g, 140 mmol) was added to a 100 mL one-neck round bottom flask and heated to 100 °C. Upon melting of the HBA-BA BOX monomer, 1,2-bis(2-aminoethoxy) ethane (11.43 g, 77 mmol) was added dropwise under vigorous stirring and left to react for 1 h. The reaction was then poured into an aluminum weigh pan and was transferred to a preheated vacuum oven. The material was allowed to react and degas for an additional hour at 120 °C under vacuum. The material was removed and cooled to room temperature to yield BAEE-iBOX as a pale yellow, tacky amorphous solid (quantitative yield, T_g = 12.72 °C). ^{1}H NMR (600 MHz, DMSO-*d*6) δ 8.13 (s, 2H, C*H*=N), 7.56 – 7.41 (m, 2H, C*H* aromatic), 7.39 – 7.28 (m, 4H, C*H* aromatic), 7.34 – 7.26 (m, 6H, C*H* aromatic), 7.29 – 7.22 (m, 2H, C*H* aromatic), 6.78 (d, *J* = 9.0 Hz, 2H, C*H* aromatic), 4.89 (s, 4H, O-CH_2-N), 3.92 (s, 4H Ar-CH_2-N), 3.83 (s, 4H Ar-CH_2-N), 3.74 – 3.53 (m, 8H, O-CH_2-CH_2-N), 3.49 – 3.44 (m, 4H, O-CH_2-CH_2-O).

Synthesis of MXDA linked imine benzoxazine (MXDA-iBOX)

HBA-BA (37.97 g, 150 mmol) was added to a 100 mL one-neck round bottom flask and heated to 100 °C. Upon melting of the HBA-BA BOX monomer, m-xylylenediamine (11.22 g, 82 mmol) was added dropwise under vigorous stirring and left to react for 1 h. The reaction was then poured into an aluminum weigh pan and was transferred to a preheated vacuum oven. The material was allowed to react and degas for an additional hour at 120 °C under vacuum. The material was removed and cooled to room temperature to yield D400-iBOX as a pale yellow, amorphous glass (quantitative yield, T_g = 40.07 °C). ^{1}H NMR (600 MHz, DMSO-d_6) δ 8.34 (s, 2H, C*H*=N), 7.53 (dd, *J* = 8.4, 2.2 Hz, 2H, C*H* aromatic), 7.41 (s, 1H, C*H* aromatic), 7.37 – 7.31 (m, 4H, C*H* aromatic), 7.33 – 7.29 (m, 5H, C*H* aromatic), 7.29 – 7.21 (m, 4H, C*H* aromatic), 7.18 (dd, *J* = 7.4, 2.2 Hz, 2H, C*H* aromatic), 6.82 (d, *J* = 8.6 Hz, 2H, C*H* aromatic), 4.91 (s, 4H, O-CH_2-N), 4.67 (s, 4H, CH_2-N=C), 3.93 (s, 4H Ar-CH_2-N), 3.83 (s, 4H Ar-CH_2-N).

.

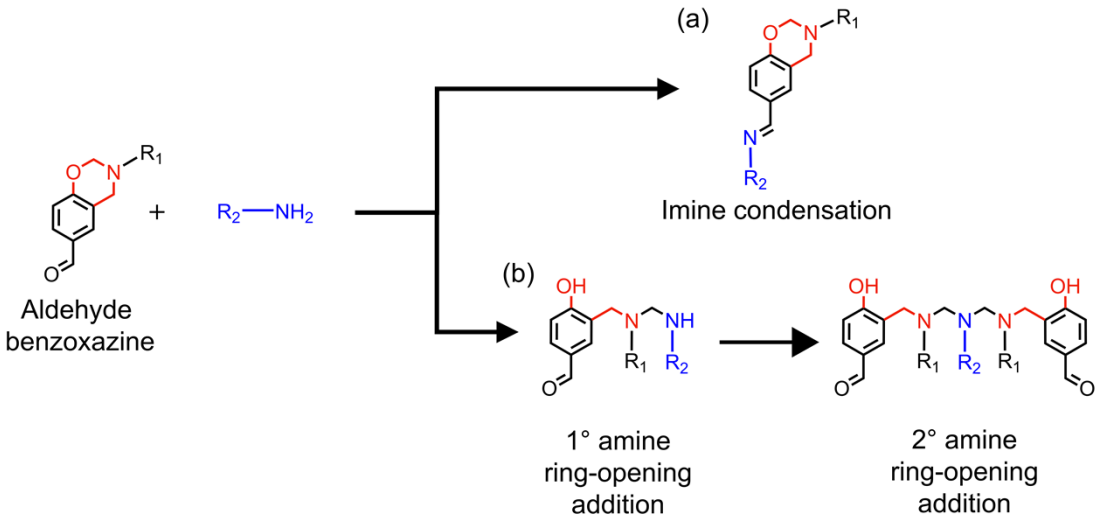

Scheme S1. Reaction pathways of aldehyde BOX and amine to yield: (a) the imine condensation product, and (b) the ring-opening addition product.

NMR Spectroscopy:

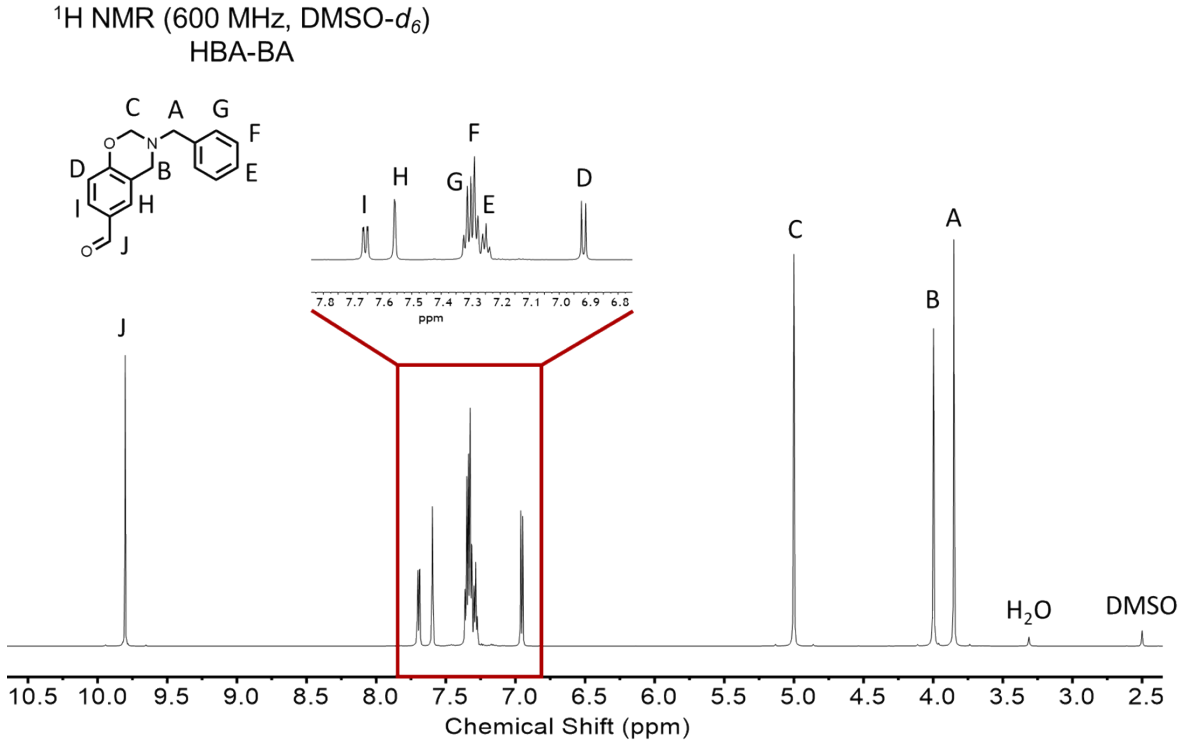

Figure S1. ^{1}H NMR spectrum of HBA-BA benzoxazine monomer.

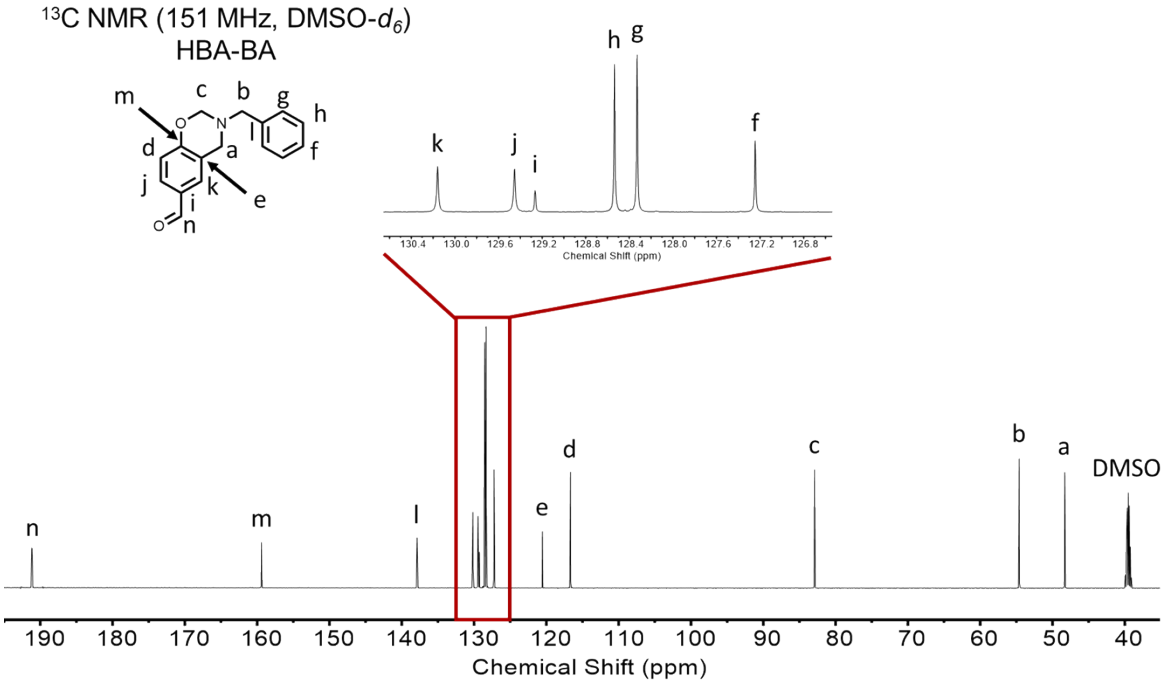

Figure S2. ^{13}C NMR spectrum of HBA-BA benzoxazine monomer**.**

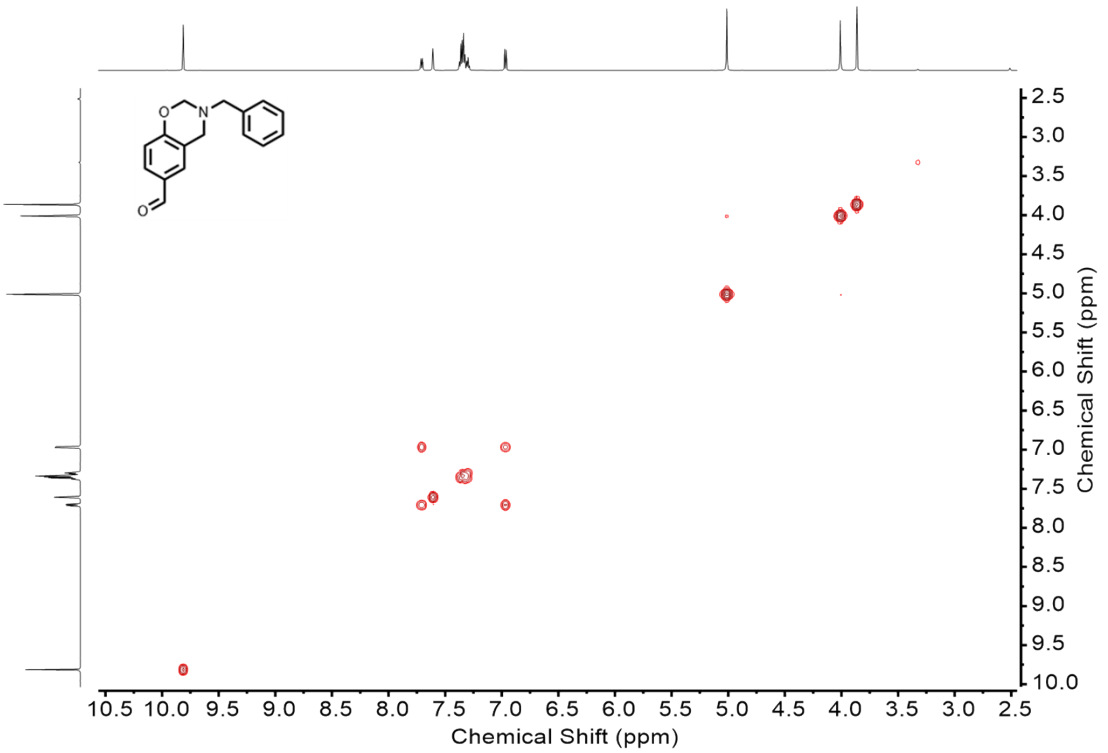

Figure S3. COSY NMR spectrum of HBA-BA benzoxazine monomer.

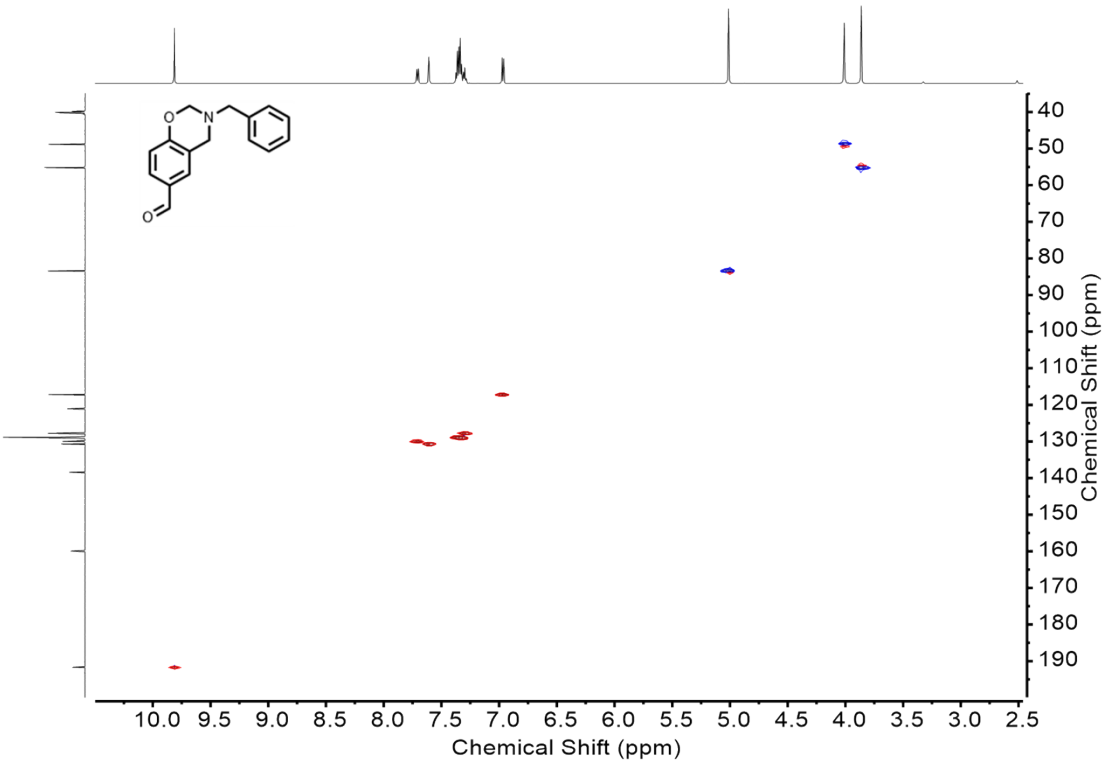

Figure S4. HSQC NMR spectrum of HBA-BA benzoxazine monomer.

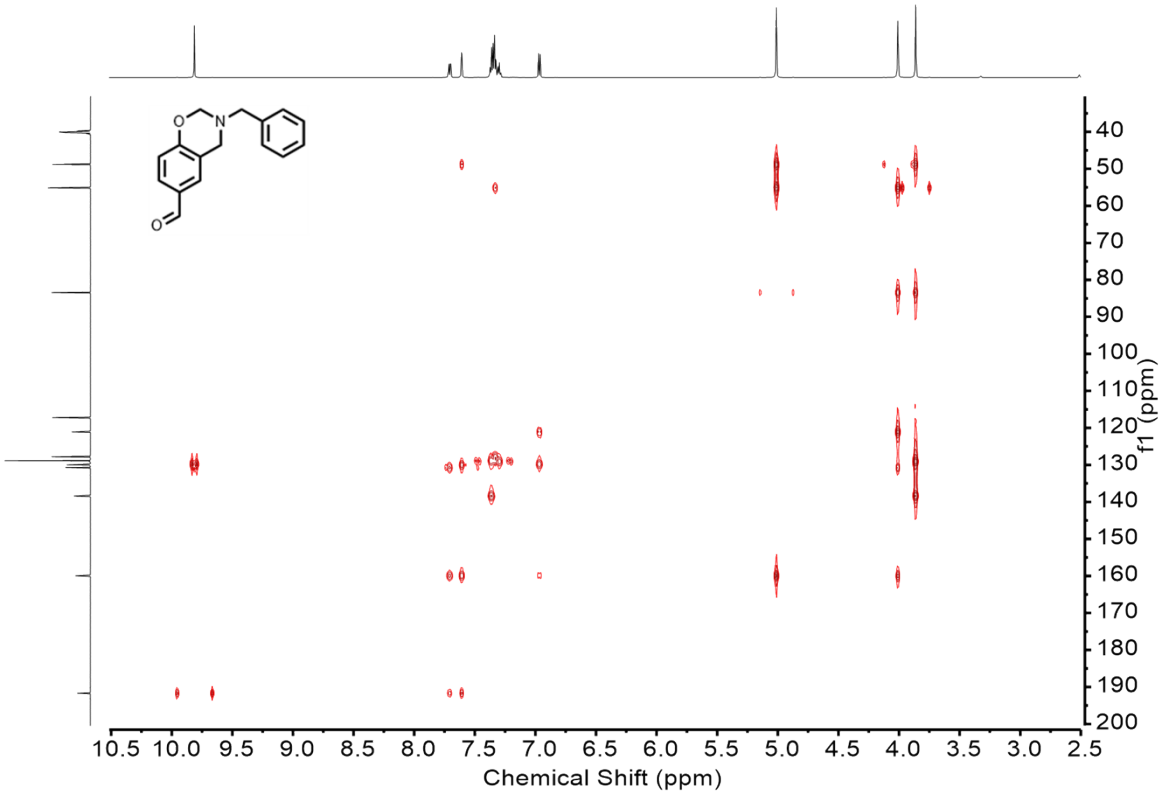

Figure S5. HMBC NMR spectrum of HBA-BA benzoxazine monomer.

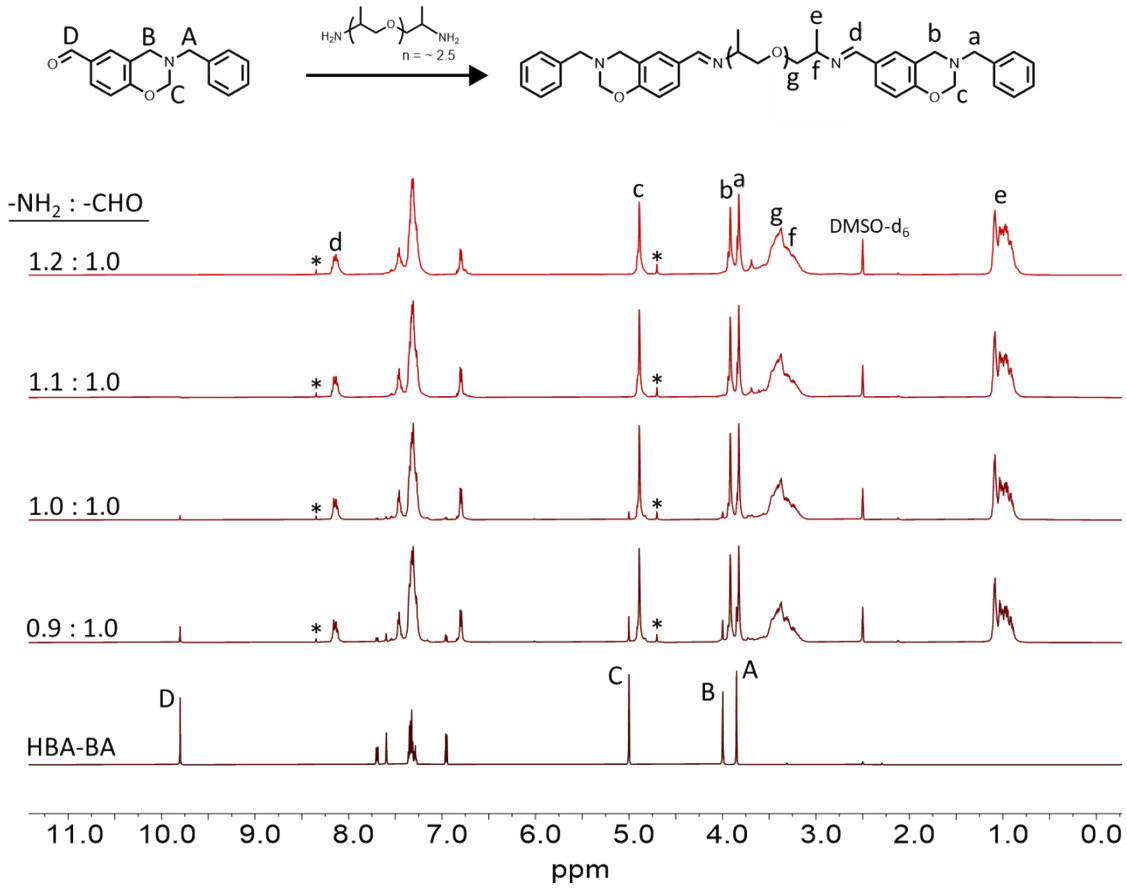

Figure S6. Stacked ^{1}H NMR spectra of D230-iBOX prepared with different stoichiometric ratios of NH_2 to CHO (* indicates presence of ring opened species resulting from ring-opening addition of $–NH_2$ to oxazine).

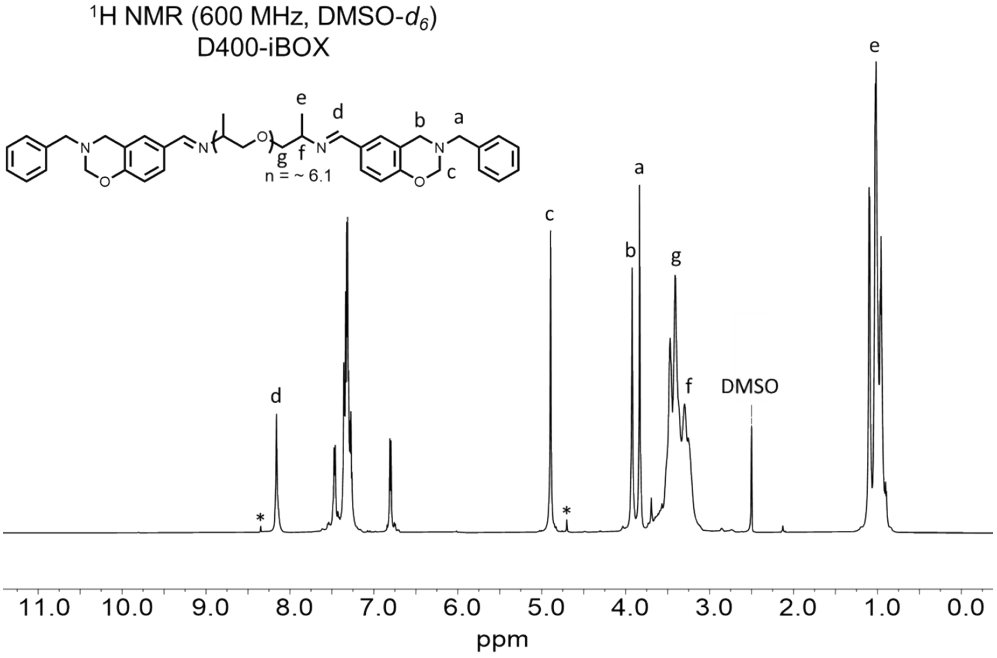

Figure S7. ¹H NMR spectrum of D400-iBOX monomer.

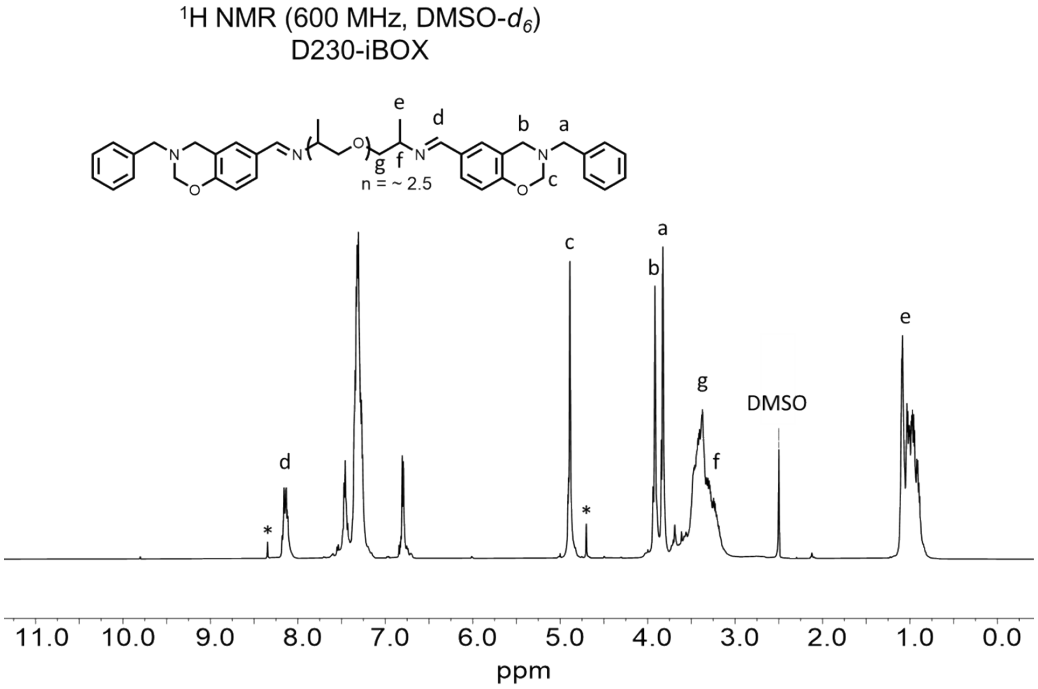

Figure S8. ¹H NMR spectrum of D230-iBOX monomer.

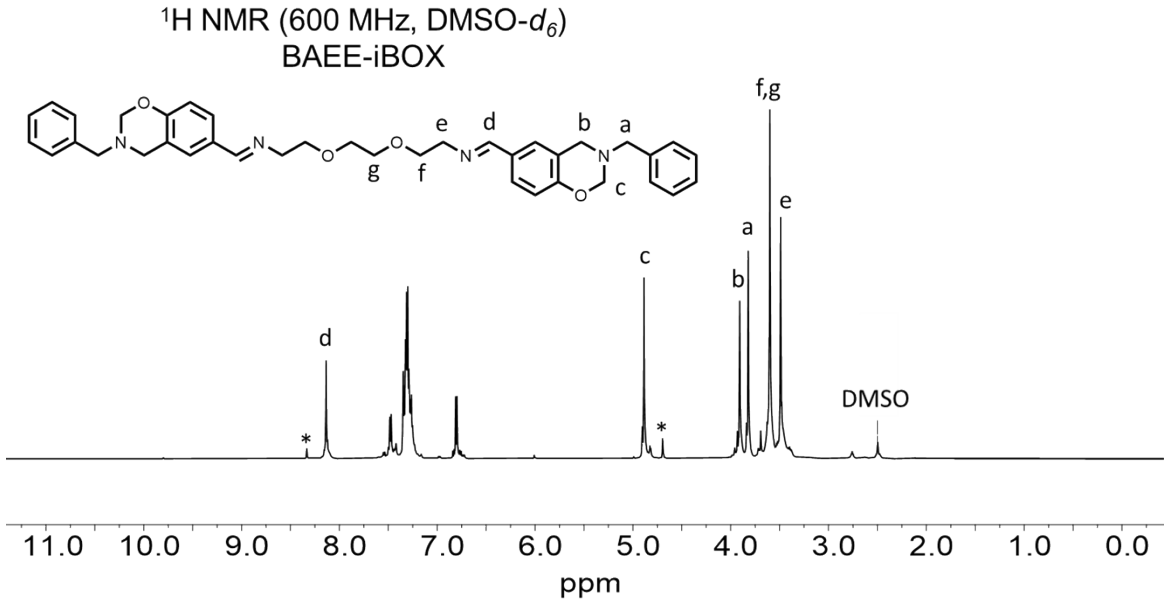

Figure S9. ¹H NMR spectrum of BAEE-iBOX monomer.

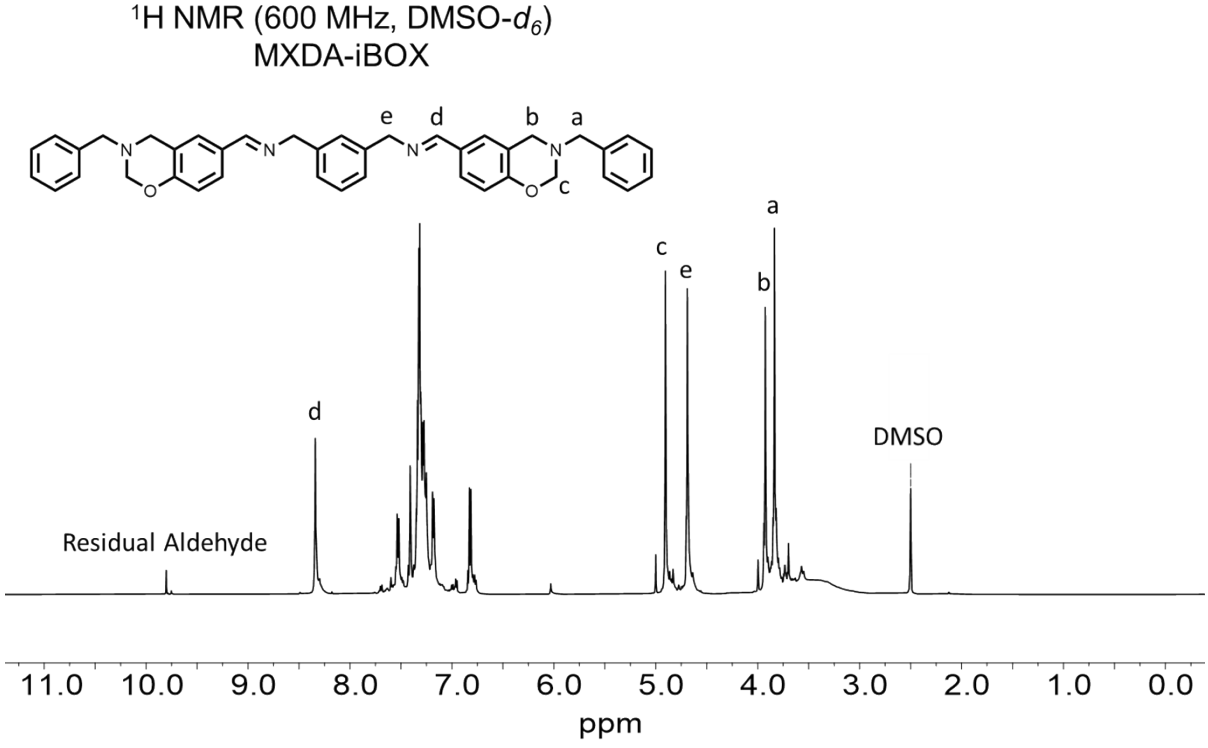

Figure S10. ¹H NMR spectrum of MXDA-iBOX monomer.

Differential Scanning Calorimetry:

Table S1. Summary of DSC results for HBA-BA and iBOX monomers

Sample	T_g (°C)	$T_{p,\ exo\ 1}$ (°C)	$T_{p,\ exo\ 2}$ (°C)
HBA-BA	55.17 (T_m)	215.01	--
D400-iBOX	-16.80	205.41	249.85
D230-iBOX	9.35	203.10	250.47
BAEE-iBOX	12.72	188.03	246.86
MXDA-iBOX	40.07	196.97	252.15

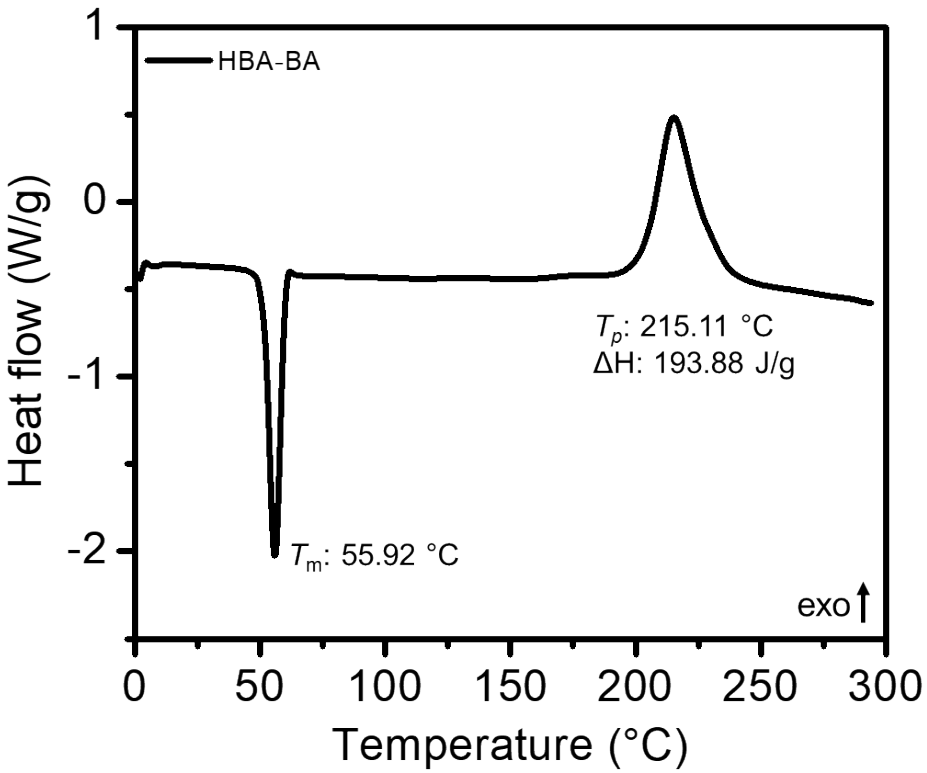

Figure S11. DSC thermogram of HBA-BA monomer (5 °C/min, N_2 atmosphere).

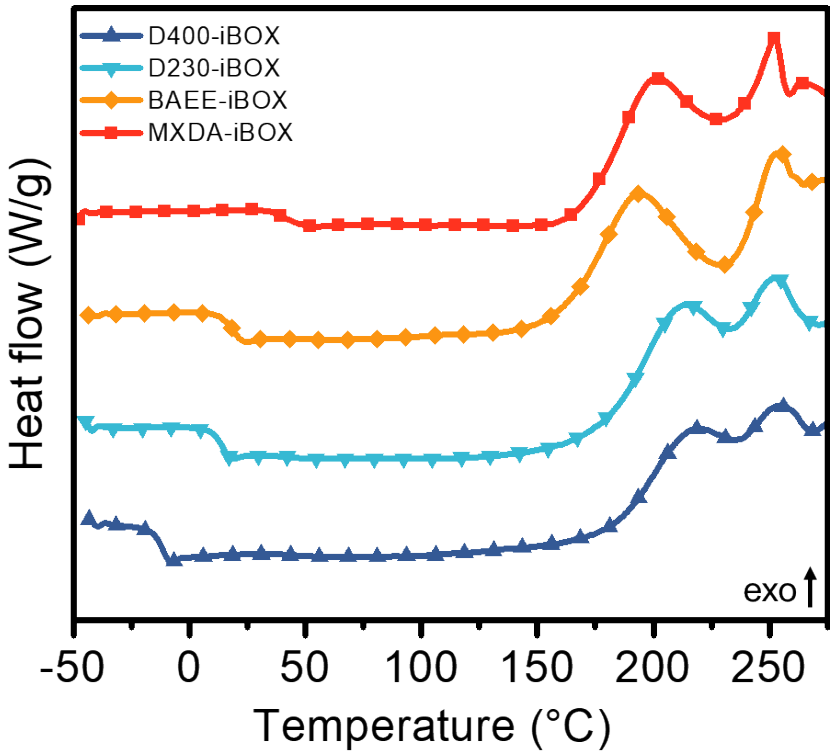

Figure S12. DSC thermogram of iBOX monomers (5 °C/min, N_2 atmosphere).

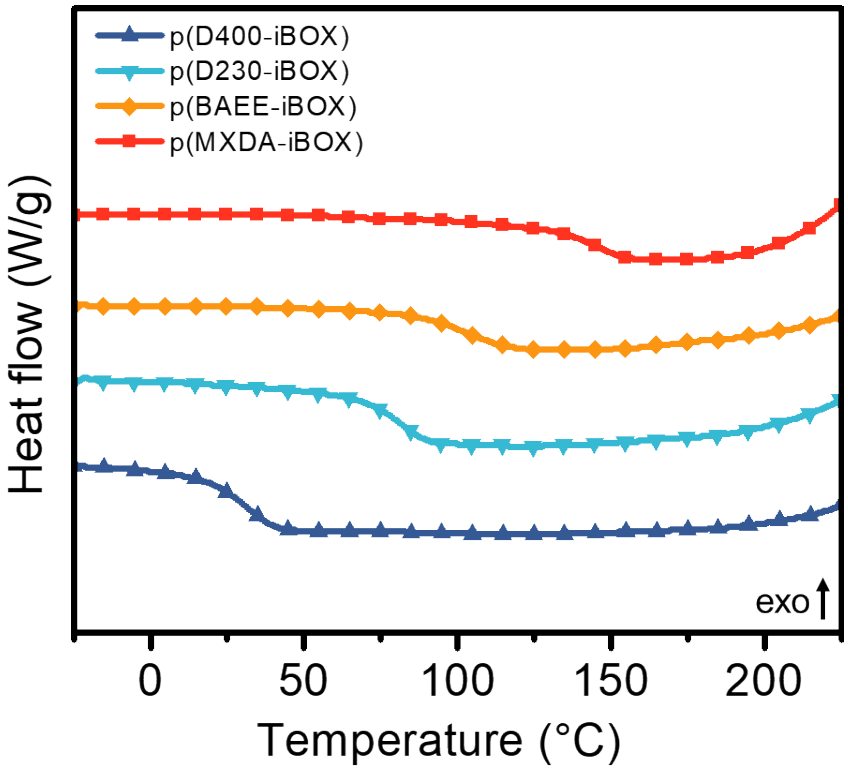

Figure S13. DSC thermogram of polymerized iBOX networks (5 °C/min, N_2 atmosphere).

Rheology:

Table S2. Summary of rheological properties of iBOX monomers

Sample	Viscosity at 50 °C (Pa·s)	Minimum viscosity (Pa·s)	Gelation temperature (°C) **
D400-iBOX	10.05	< 0.5*	174.4
D230-iBOX	313.6	< 0.5*	168.8
BAEE-iBOX	1130	< 0.5*	149.5
MXDA-iBOX	> 10^5	3.67 (147 °C)	161.9

* Beyond detection limit of employed geometry/strain
** Determined by storage/loss modulus crossover

FTIR Spectroscopy:

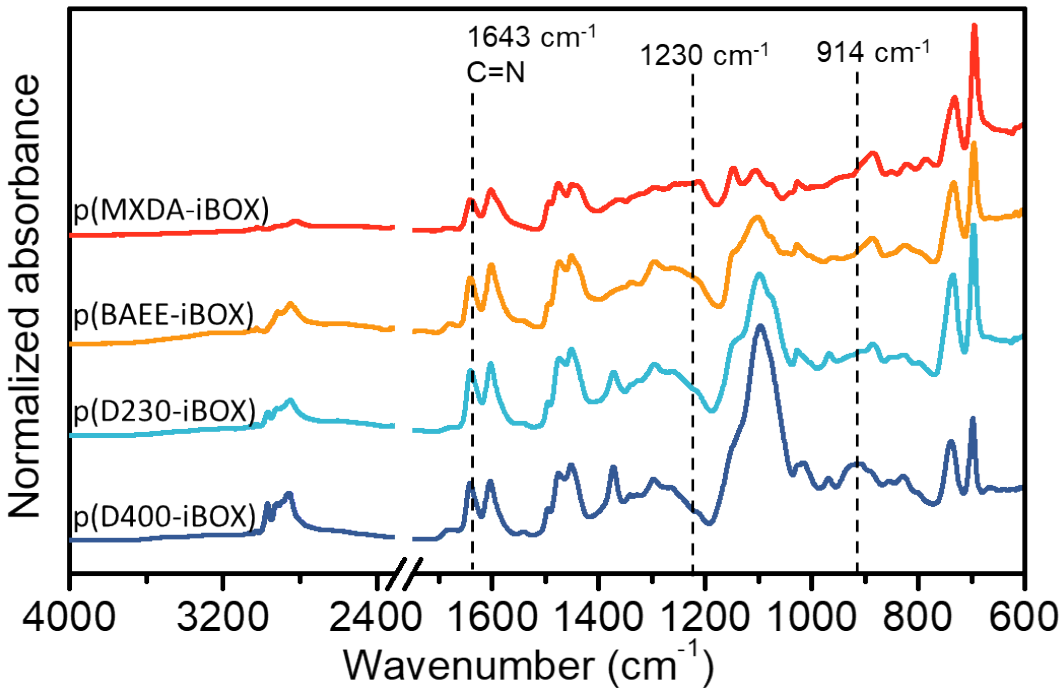

Figure S14. FTIR spectra of p(iBOX) networks after polymerizing at 180 °C for 2 hours.

Thermogravimetric Analysis:

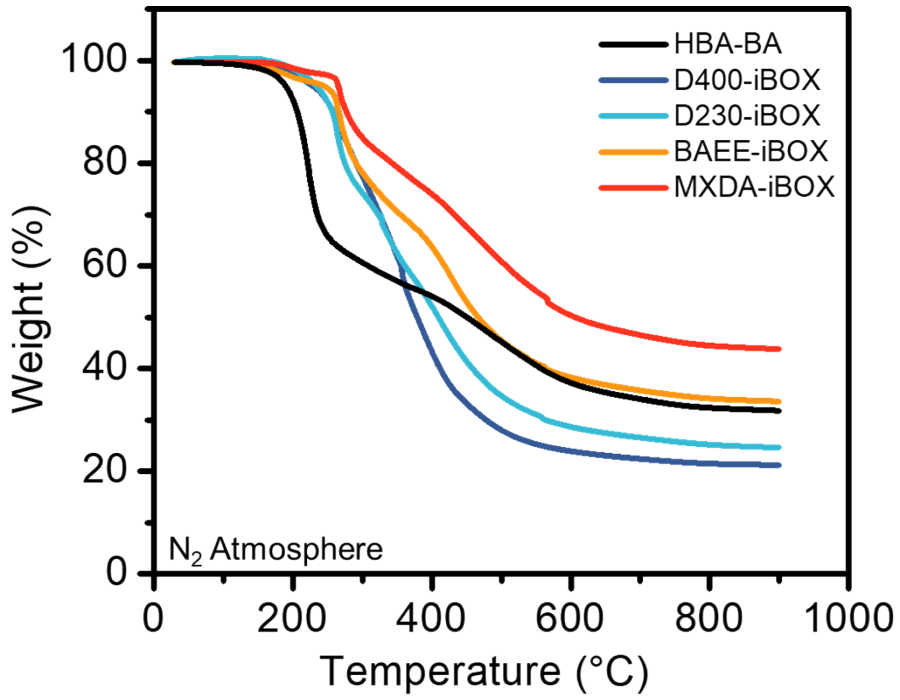

Figure S15. TGA thermogram of benzoxazine monomers (10 °C/min, N_2 atmosphere).

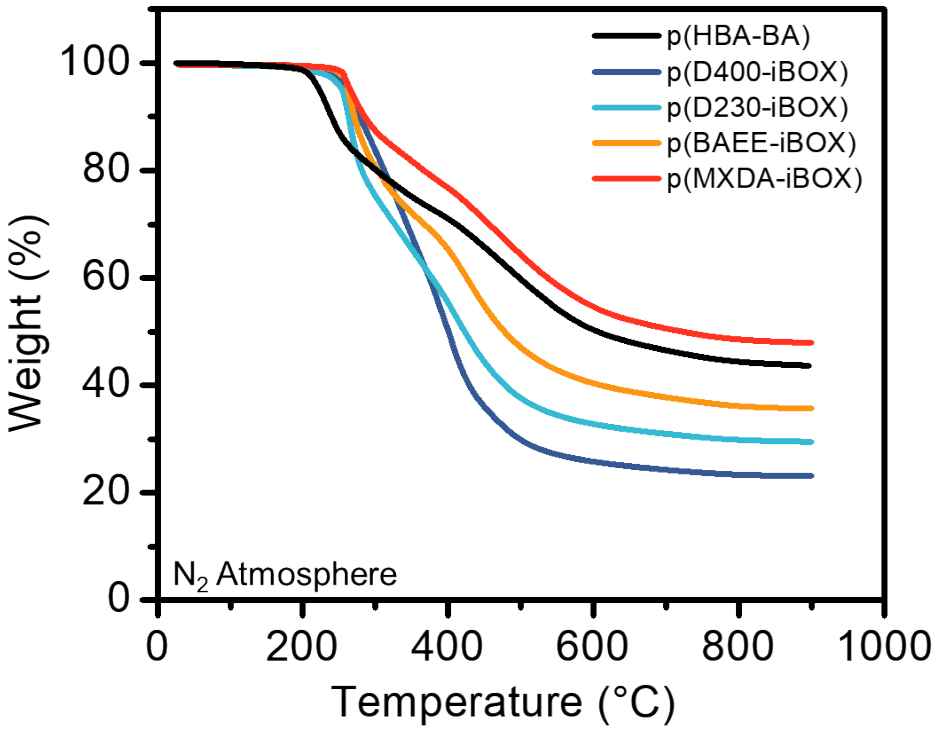

Figure S16. TGA thermogram of polybenzoxazine networks (10 °C/min, N_2 atmosphere).

.

Table S3. Summary of TGA results in an N_2 atmosphere for BOX monomers and polymerized networks

Sample		$T_{d,\ 5\%}$ (°C)	$T_{d,\ 10\%}$ (°C)	Char yield @ 900 °C (%)
HBA-BA	Monomer	186.81	202.21	32.15
	Network	222.72	239.41	43.69
D400-iBOX	Monomer	228.39	254.52	21.56
	Network	257.90	275.18	23.44
D230-iBOX	Monomer	232.18	253.32	24.96
	Network	250.84	259.06	29.83
BAEE-iBOX	Monomer	245.03	262.12	33.95
	Network	258.54	267.40	35.99
MXDA-iBOX	Monomer	261.68	273.82	44.13
	Network	262.46	282.47	48.25

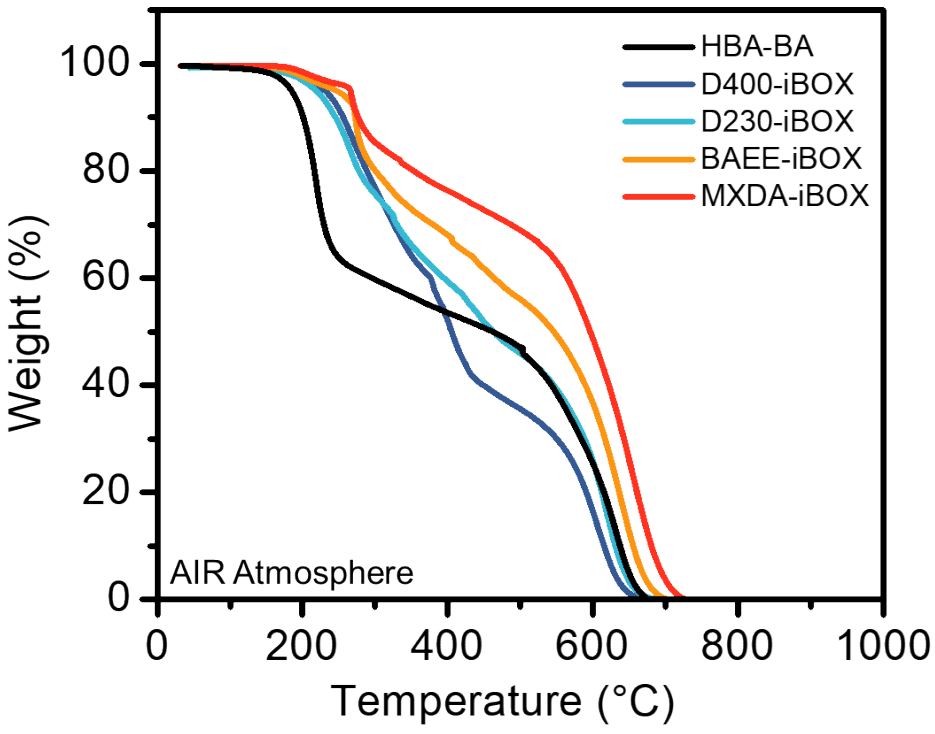

Figure S17. TGA thermogram of benzoxazine monomers (10 °C/min, AIR atmosphere).

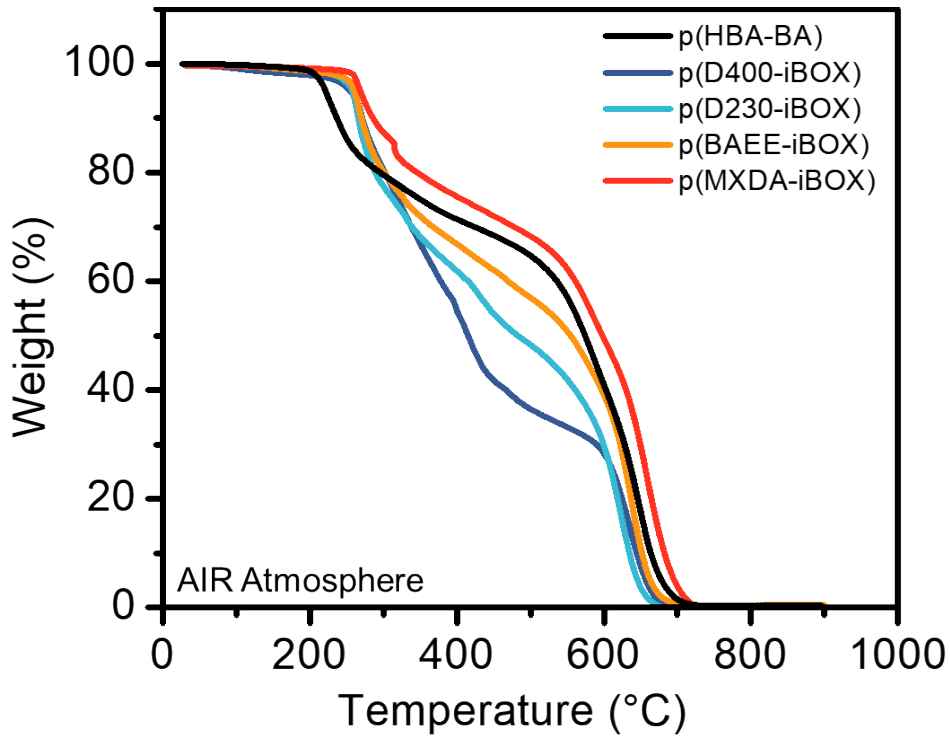

Figure S18. TGA thermogram of polybenzoxazine networks (10 °C/min, AIR atmosphere).

Table S4. Summary of TGA results in an air atmosphere for BOX monomers and polymerized networks

Sample		$T_{d,\ 5\%}$ (°C)	$T_{d,\ 10\%}$ (°C)
HBA-BA	Monomer	182.06	197.34
	Network	220.71	236.59
D400-iBOX	Monomer	229.60	253.06
	Network	252.50	267.47
D230-iBOX	Monomer	216.70	242.31
	Network	254.03	261.98
BAEE-iBOX	Monomer	246.69	268.62
	Network	256.84	266.42
MXDA-iBOX	Monomer	262.14	273.36
	Network	265.14	282.79

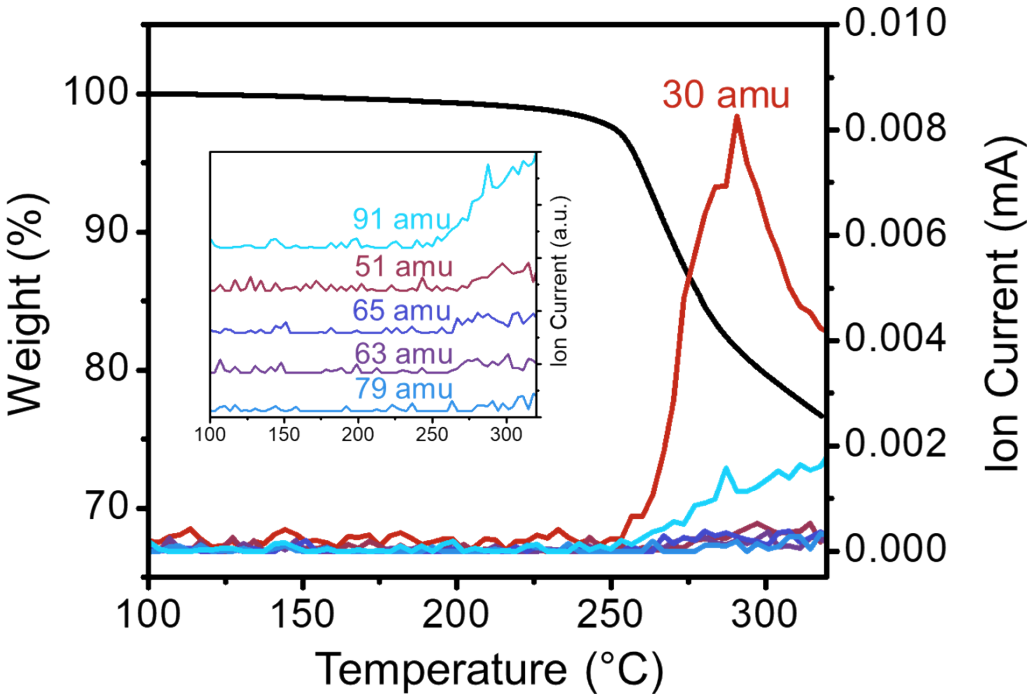

Figure S19. TGA-MS thermogram of p(BAEE-iBOX) network (10 °C/min, N_2 atmosphere). Molecular atomic mass units (amu) of evolved degradation products are shown, confirming initial degradation at the tertiary amine Mannich bridge in the network backbone resulting in volatilization of fragments of the benzylamine pendant.

Exchange Kinetics:

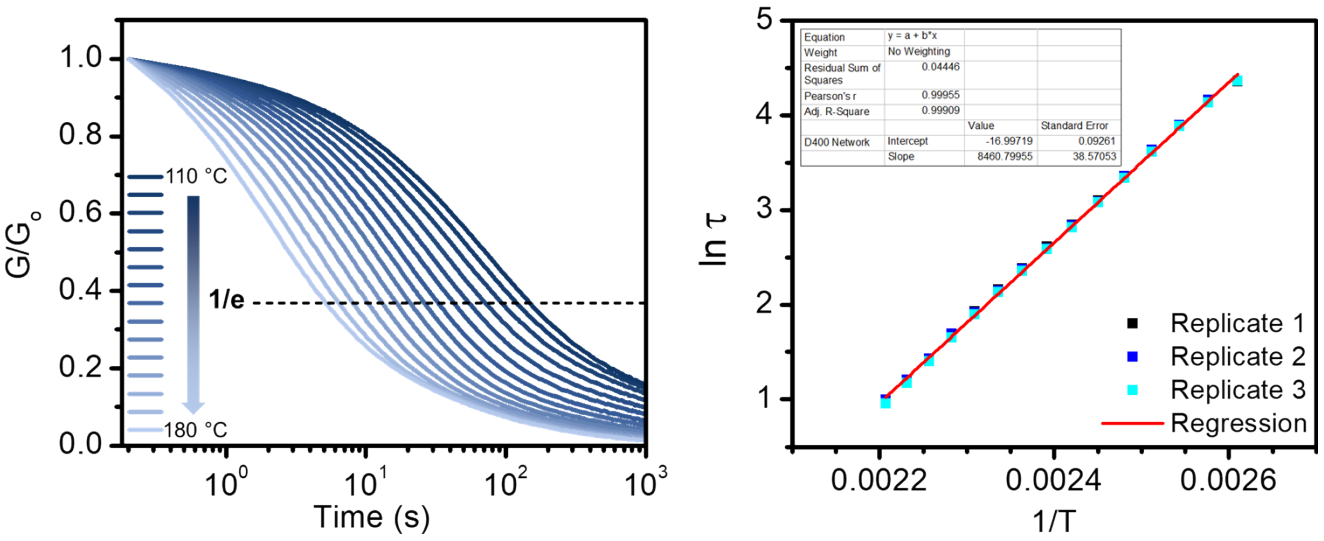

Figure S20. p(D400-iBOX) stress relaxation curves (left) and resulting Arrhenius plot (right).

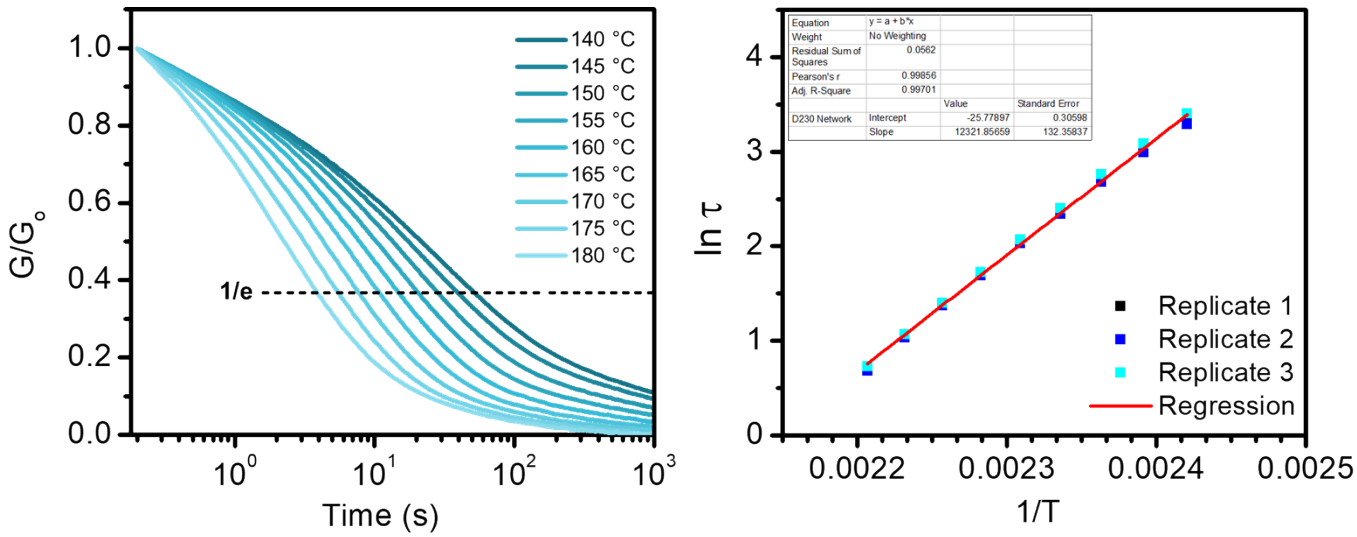

Figure S21. p(D230-iBOX) stress relaxation curves (left) and resulting Arrhenius plot (right).

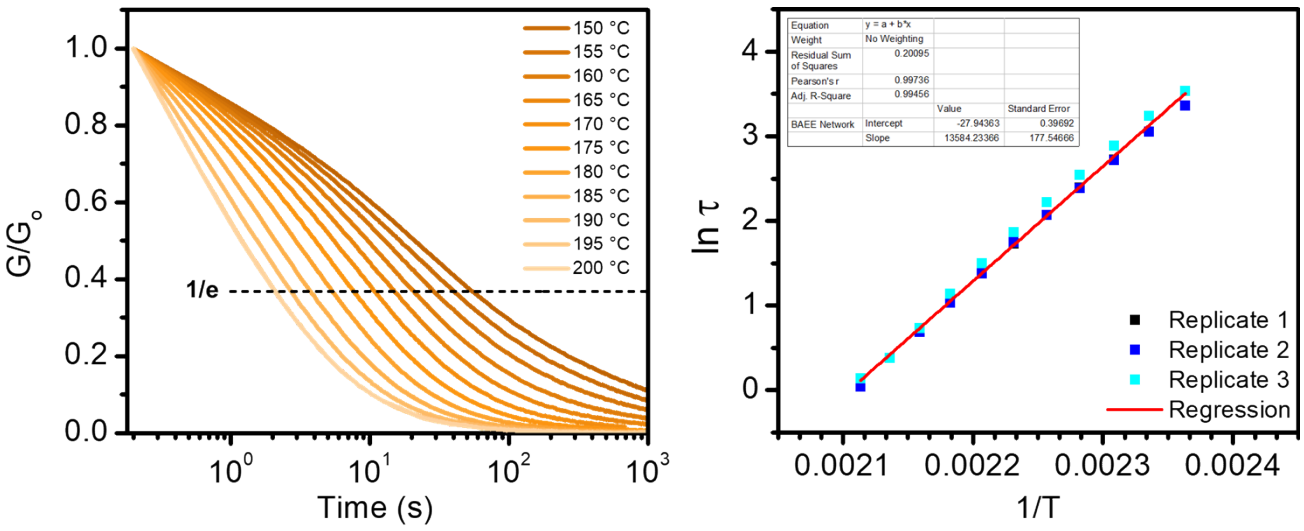

Figure S22. p(BAEE-iBOX) stress relaxation curves (left) and resulting Arrhenius plot (right).

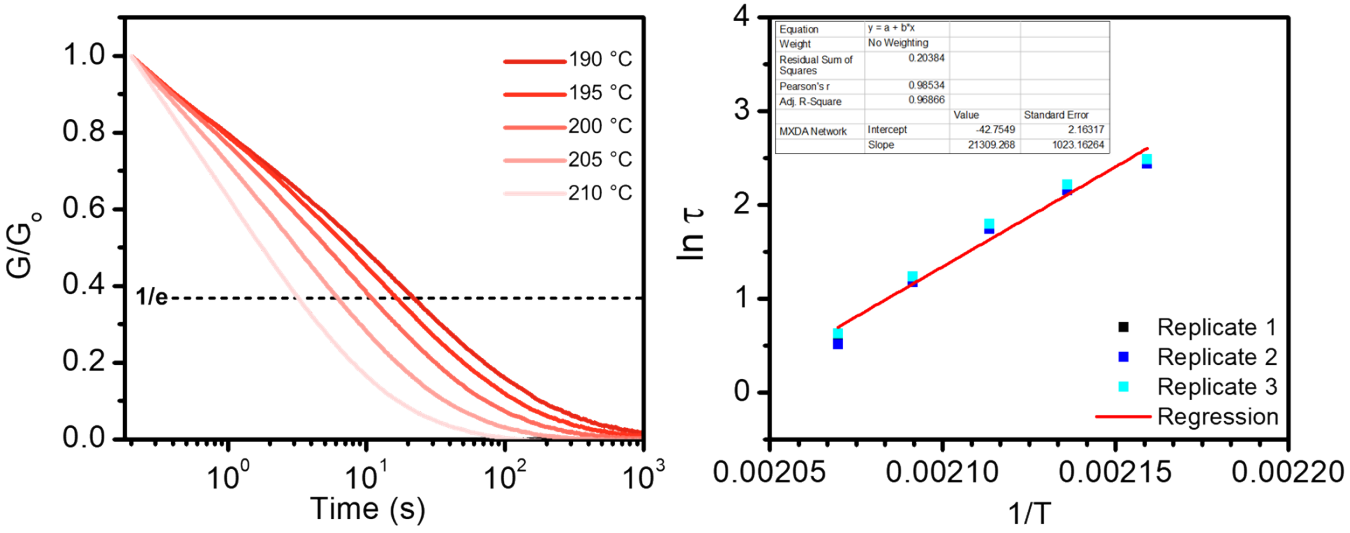

Figure S23. p(MXDA-iBOX) stress relaxation curves (left) and resulting Arrhenius plot (right).

Isothermal Creep-Recovery:

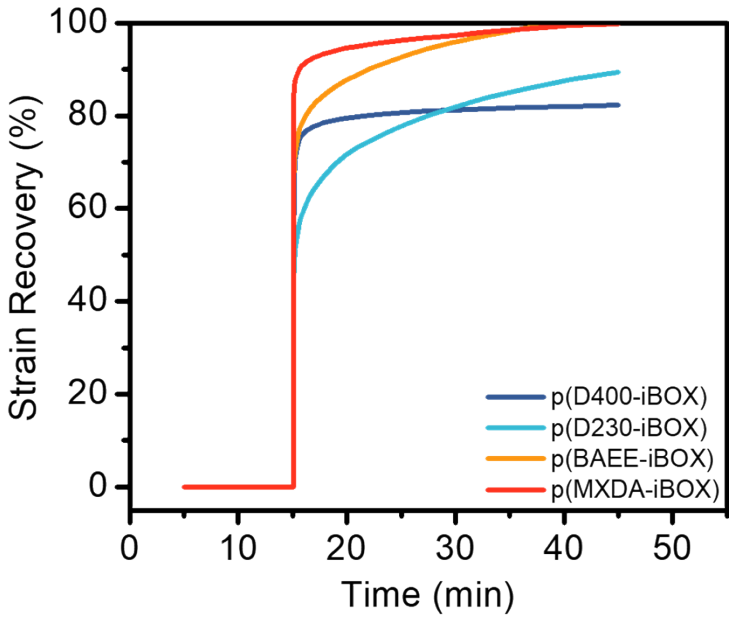

Figure S24. Creep recovery curves of p(iBOX) networks at 50 °C.

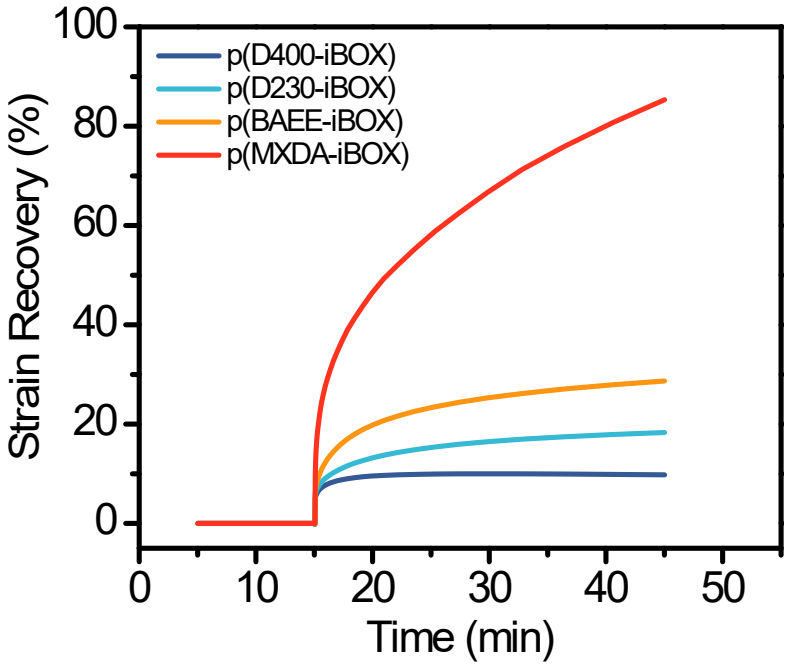

Figure S25. Creep recovery curves of p(iBOX) networks at 150 °C.

Table S5. Creep-recovery results for p(iBOX) networks conducted at 50 °C and 150°C

Vitrimer Network	50 °C, 1.0 MPa		150 °C, 0.1 MPa	
	Maximum strain (%)	Recovery (%)	Maximum strain (%)	Recovery (%)
p(D400-iBOX)	23.7	82.2	67.6	9.8
p(D230-iBOX)	0.09	89.3	26.7	18.3
p(BAEE-iBOX)	0.07	98.8	5.9	28.7
p(MXDA-iBOX)	0.03	99.8	0.22	85.3

Thermal Reprocessing:

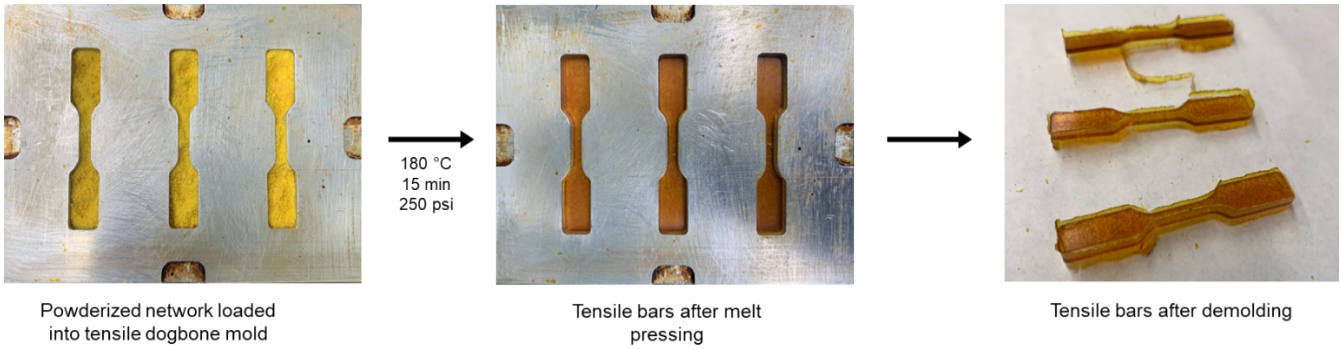

Figure S26. Images of thermal reprocessing process, showing ground p(iBOX) powder and reprocessed tensile bars.

Table S6. Summary of tensile properties for p(iBOX) networks through 3 cycles of reprocessing

Sample		Modulus (MPa)	Peak stress (MPa)	Strain at break (%)	Toughness (10^6 J/m^3)
p(D400-iBOX)	Virgin	19.08 ± 3.65	9.70 ± 0.38	265 ± 14	15.6 ± 1.2
	Reprocessed 1	21.07 ± 2.98	13.79 ± 1.07	365 ± 25	28.4 ± 3.7
	Reprocessed 2	27.88 ± 2.87	13.21 ± 0.94	319 ± 30	24.1 ± 3.0
	Reprocessed 3	25.17 ± 3.07	13.12 ± 0.49	256 ± 7	20.5 ± 0.9
p(D230-iBOX)	Virgin	806.3 ± 21.4	70.1 ± 0.5	15.3 ± 0.6	7.1 ± 0.3
	Reprocessed 1	719.9 ± 26.0	53.9 ± 5.6	9.5 ± 1.3	2.9 ± 0.8
	Reprocessed 2	783.1 ± 19.1	45.4 ± 1.5	6.6 ± 0.2	1.6 ± 0.1
	Reprocessed 3	820.7 ± 13.2	38.2 ± 5.6	5.2 ± 0.9	1.1 ± 0.4
p(BAEE-iBOX)	Virgin	883.7 ± 26.9	79.5 ± 2.1	11.9 ± 0.5	5.6 ± 0.4
	Reprocessed 1	874.1 ± 29.9	56.3 ± 8.7	9.1 ± 1.5	3.1 ± 0.9
	Reprocessed 2	922.6 ± 10.2	52.7 ± 4.9	8.2 ± 1.1	2.4 ± 0.6
	Reprocessed 3	896.2 ± 26.5	54.2 ± 2.1	8.5 ± 0.5	2.4 ± 0.2
p(MXDA-iBOX)	Virgin	989.2 ± 33.0	70.3 ± 2.8	8.4 ± 0.5	3.3 ± 0.3
	Reprocessed 1	926.0 ± 28.8	49.3 ± 4.1	6.0 ± 0.9	1.5 ± 0.4
	Reprocessed 2	1014 ± 17	27.2 ± 4.2	3.0 ± 0.6	0.4 ± 0.2
	Reprocessed 3	1034 ± 36	19.9 ± 4.7	2.2 ± 0.7	0.3 ± 0.1

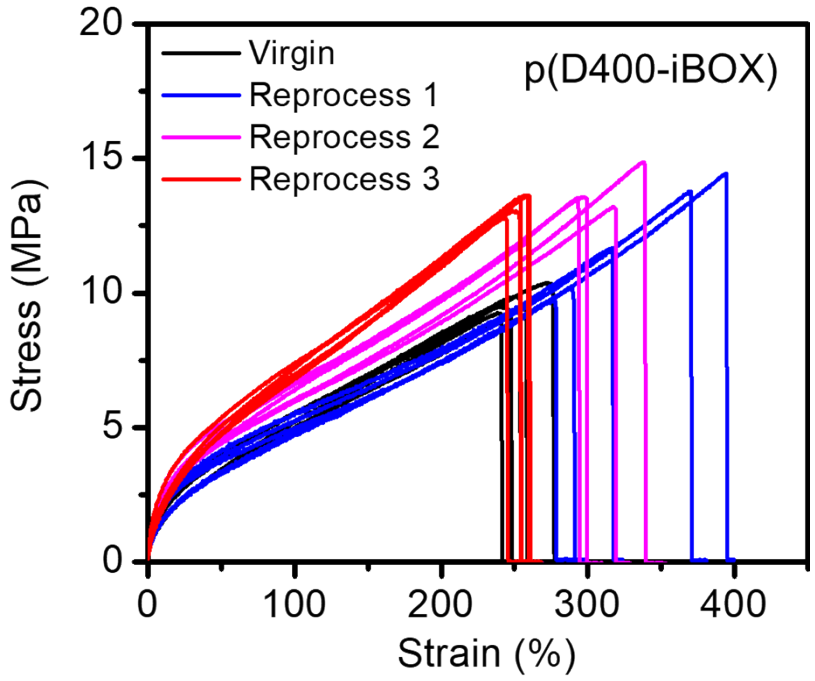

Figure S27. Stress vs. strain curves for p(D400-iBOX) through 3 reprocessing cycles.

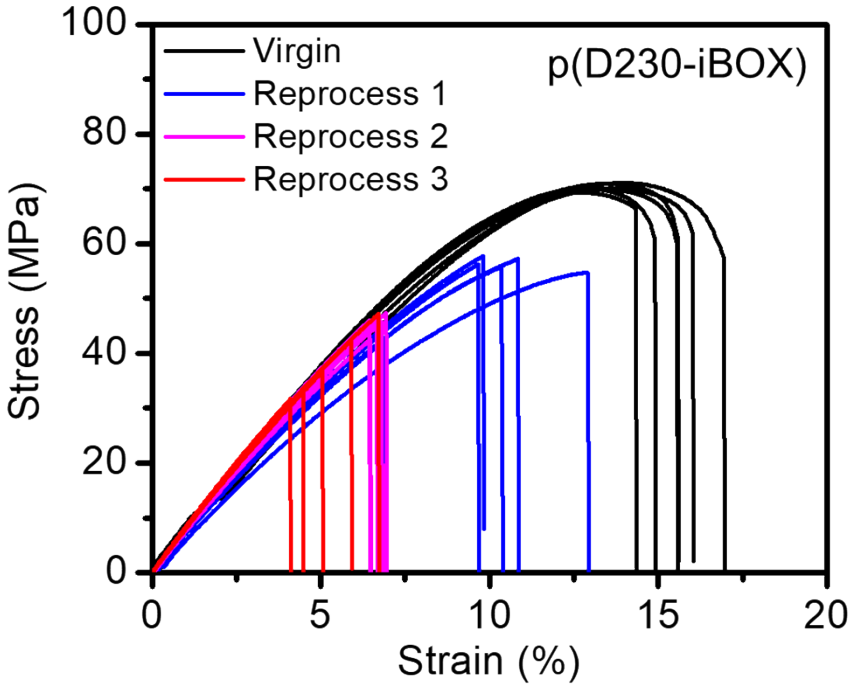

Figure S28. Stress vs. strain curves for p(D230-iBOX) through 3 reprocessing cycles.

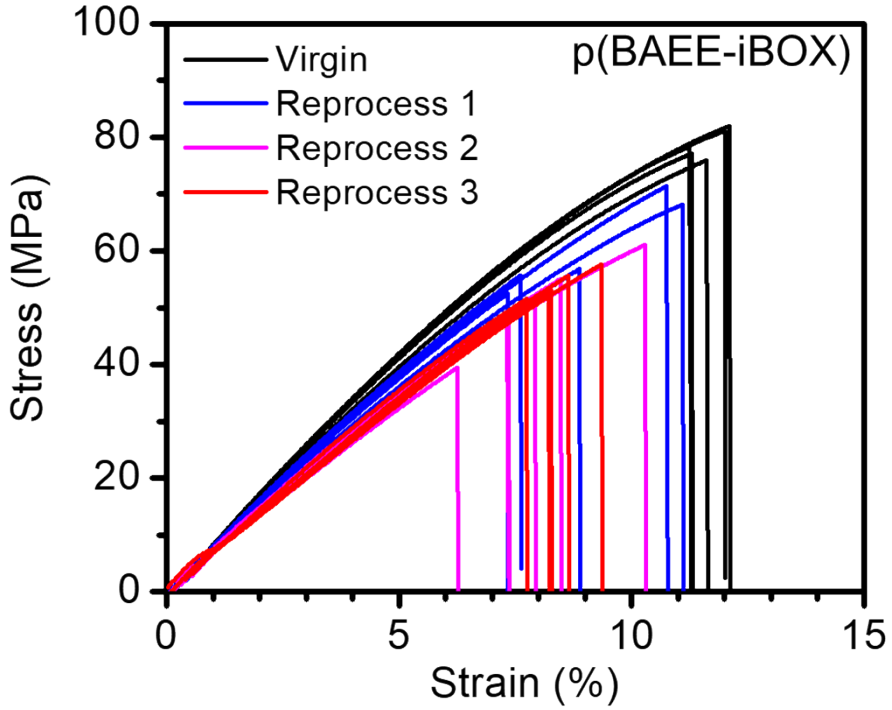

Figure S29. Stress vs. strain curves for p(BAEE-iBOX) through 3 reprocessing cycles.

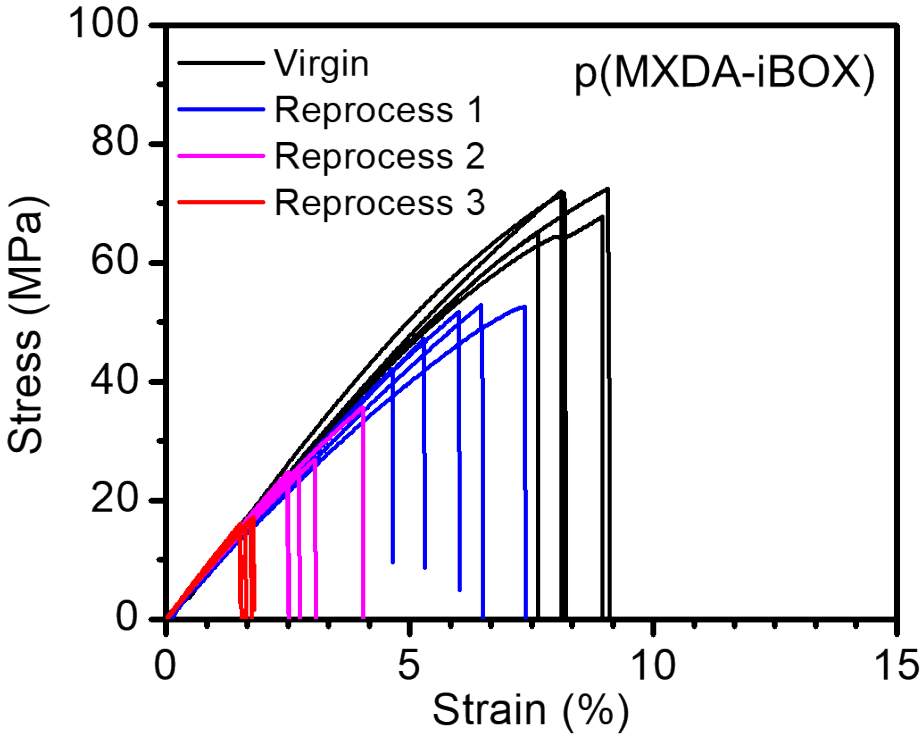

Figure S30. Stress vs. strain curves for p(MXDA-iBOX) through 3 reprocessing cycles.

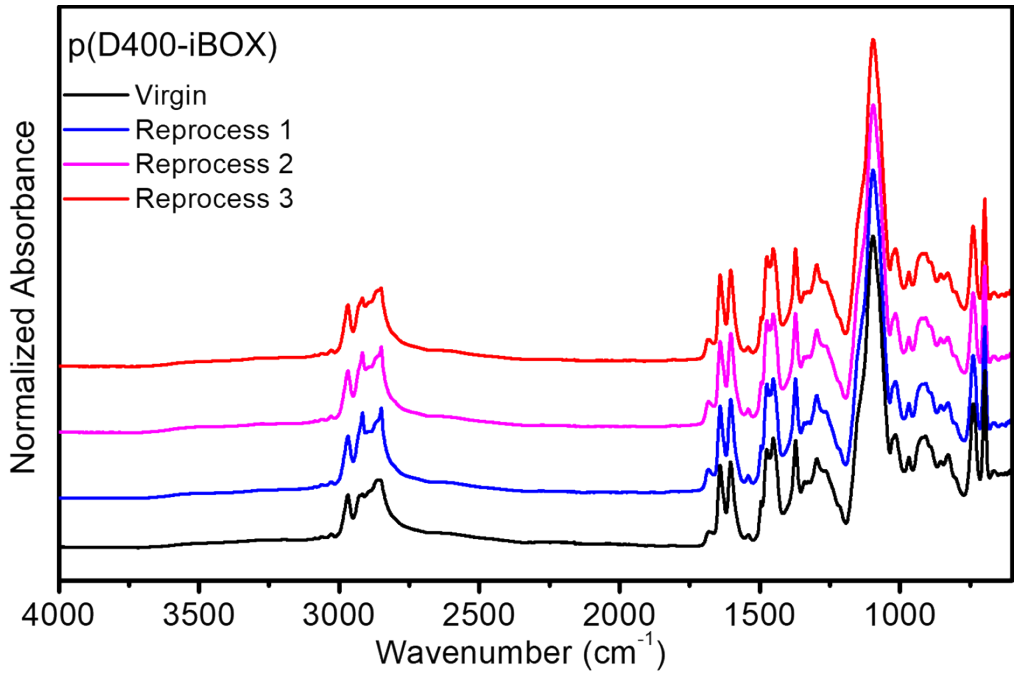

Figure S31. FTIR spectra of p(D400-iBOX) through 3 reprocessing cycles.

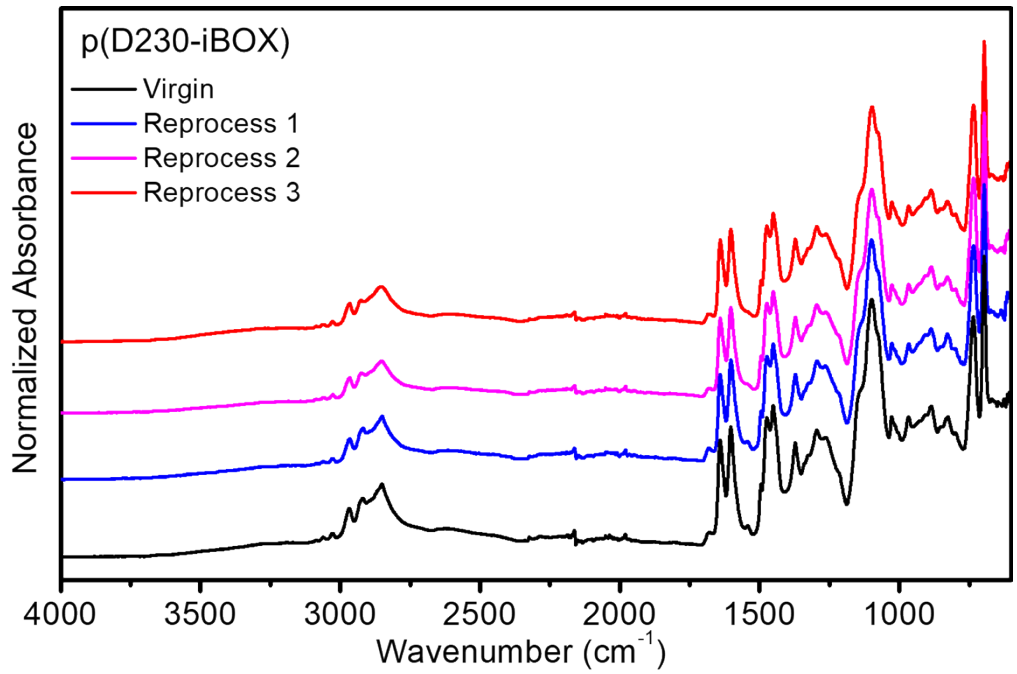

Figure S32. FTIR spectra of p(D230-iBOX) through 3 reprocessing cycles.

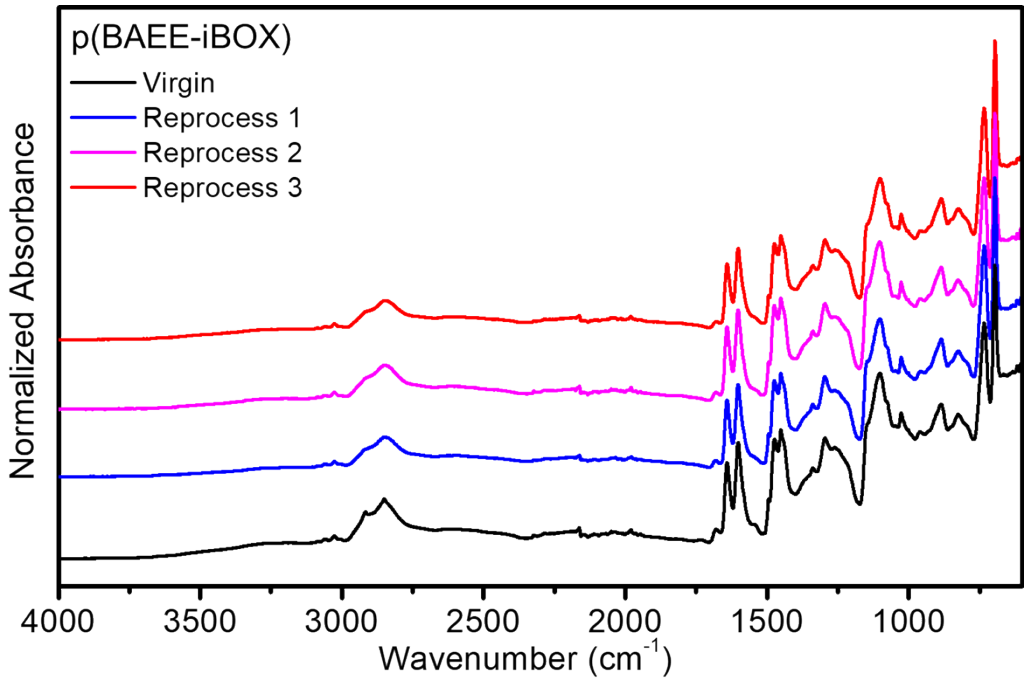

Figure S33. FTIR spectra of p(BAEE-iBOX) through 3 reprocessing cycles.

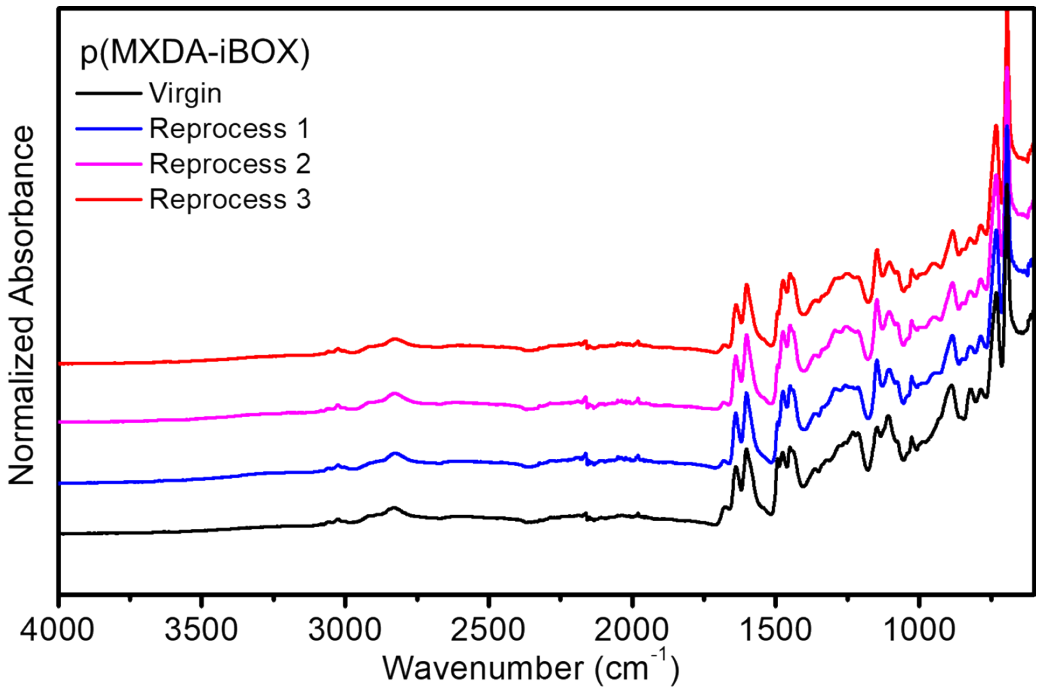

Figure S34. FTIR spectra of p(BAEE-iBOX) through 3 reprocessing cycles.

Self-Healing:

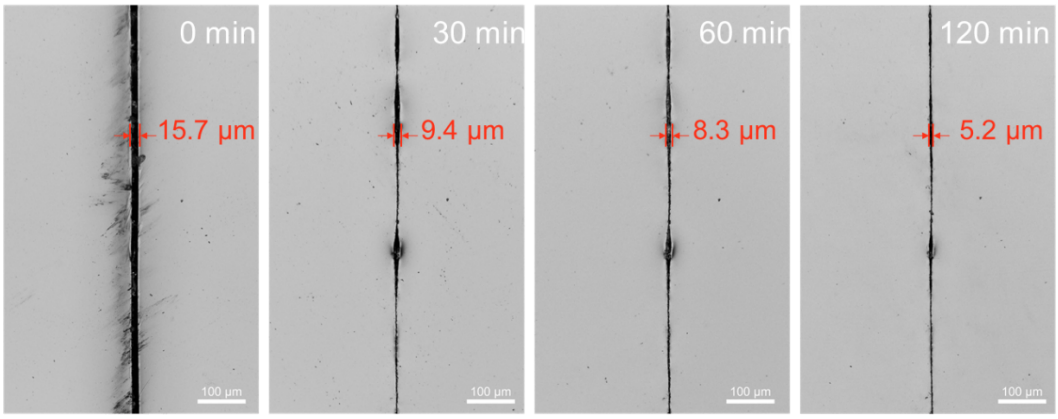

Figure S35. Scratch healing of p(D400-iBOX) network after eating at 180 °C for various times.

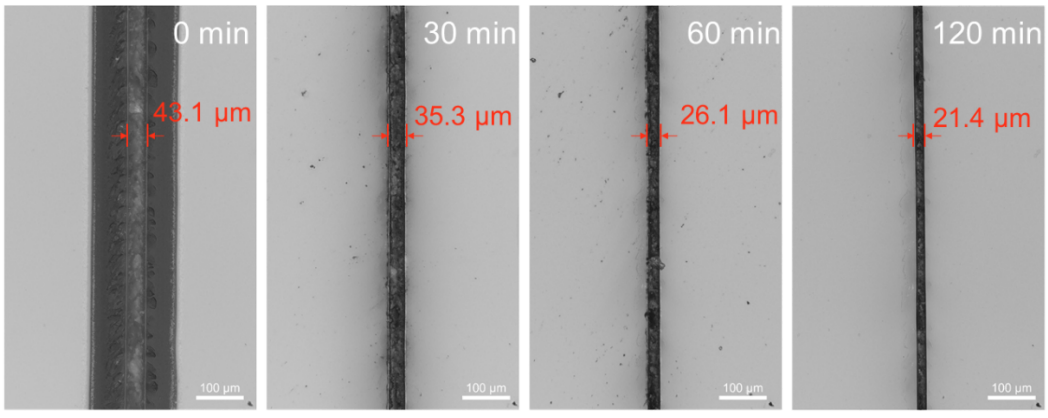

Figure S36. Scratch healing of p(D230-iBOX) network after eating at 180 °C for various times.

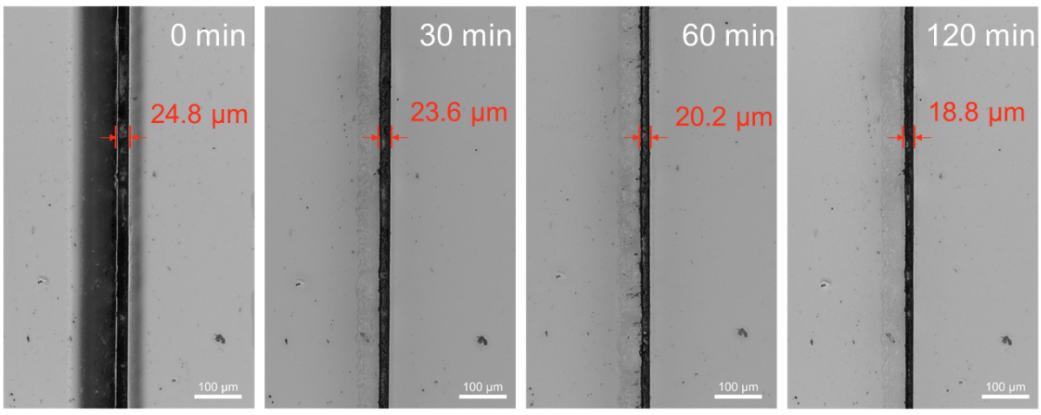

Figure S37. Scratch healing of p(BAEE-iBOX) network after eating at 180 °C for various times.

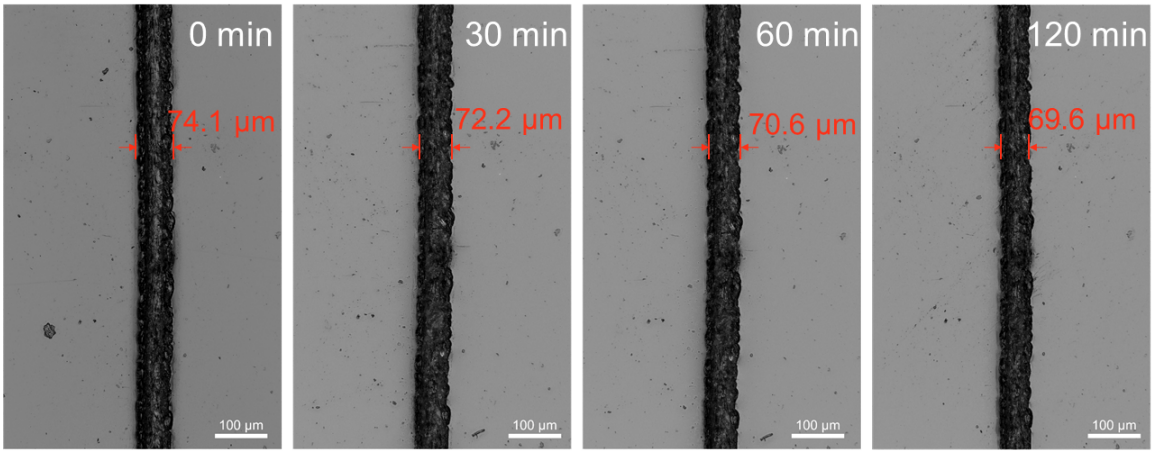

Figure S38. Scratch healing of p(MXDA-iBOX) network after eating at 180 °C for various times.

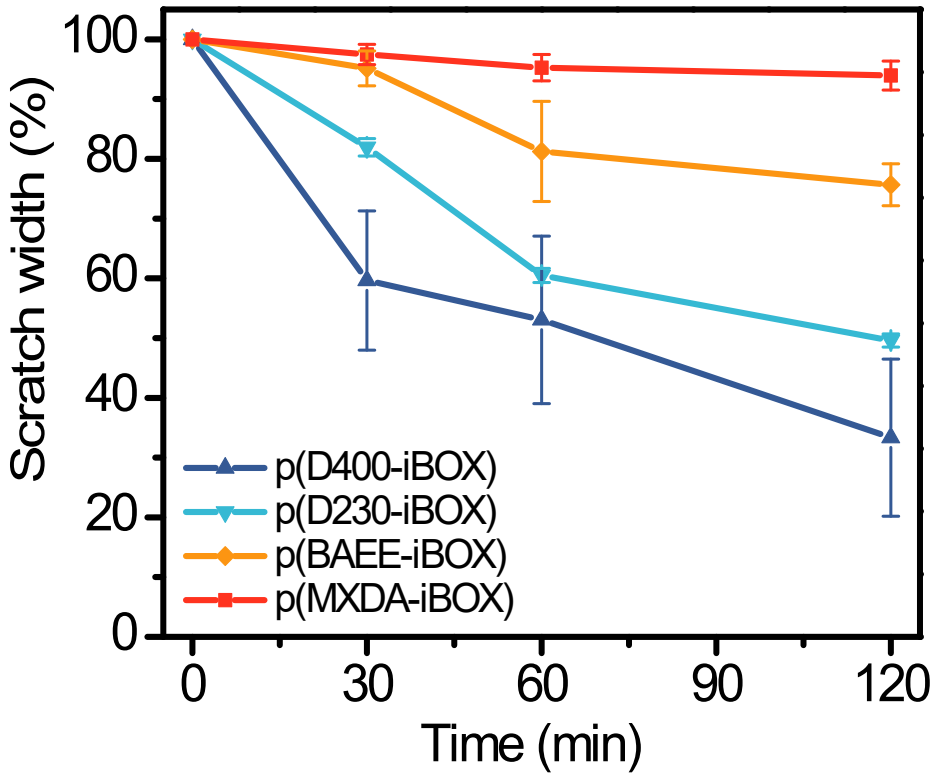

Figure S39. Scratch width vs. time at 180 °C for all p(iBOX) networks.

Solvent Stability & Chemical Degradation:

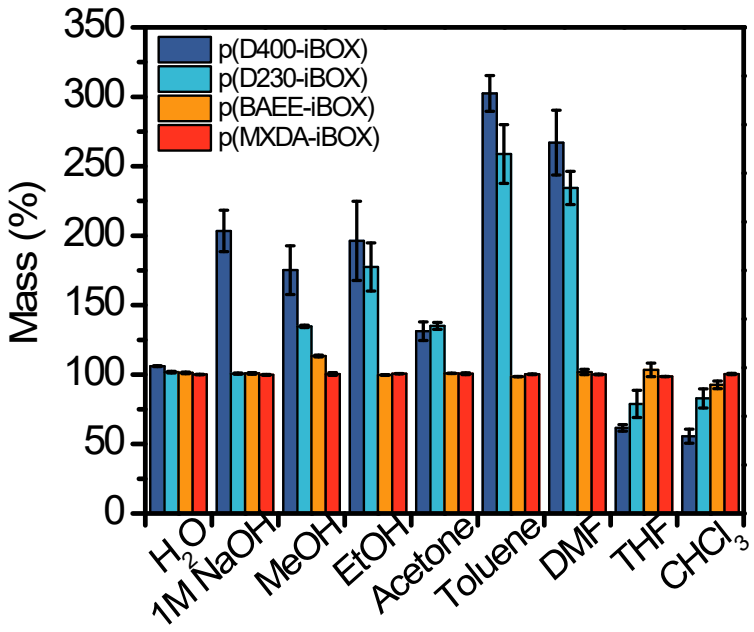

Figure S40. Mass change of p(iBOX) networks in various solvents at 25 °C for 7 days.

Table S7. Summary of mass change of p(iBOX) networks after 7 days of solvent exposure 25 °C

Solvent	Network			
	p(D400-iBOX)	p(D230-iBOX)	p(BAEE-iBOX)	p(MXDA-iBOX)
H_2O	106.1 ± 0.4	101.8 ± 0.6	101.3 ± 0.6	100.1 ± 0.2
1M NaOH	203.4 ± 14.9	100.7 ± 0.4	100.9 ± 0.6	99.8 ± 0.3
MeOH	175.2 ± 17.5	134.7 ± 0.9	113.3 ± 0.6	100.4 ± 1.0
EtOH	196.3 ± 28.5	177.5 ± 17.4	99.7 ± 0.3	100.7 ± 0.13
Acetone	131.2 ± 6.7	135.1 ± 2.5	100.9 ± 0.1	100.6 ± 0.7
Toluene	302.5 ± 12.9	258.8 ± 21.1	98.6 ± 0.1	100.2 ± 0.3
DMF	267.0 ± 23.3	234.4 ± 12.0	101.9 ± 1.9	100.1 ± 0.3
THF	61.6 ± 2.3	78.9 ± 9.8	103.4 ± 4.9	98.6 ± 0.1
$CHCl_3$	55.6 ± 5.0	82.8 ± 6.9	92.6 ± 2.7	100.4 ± 0.2

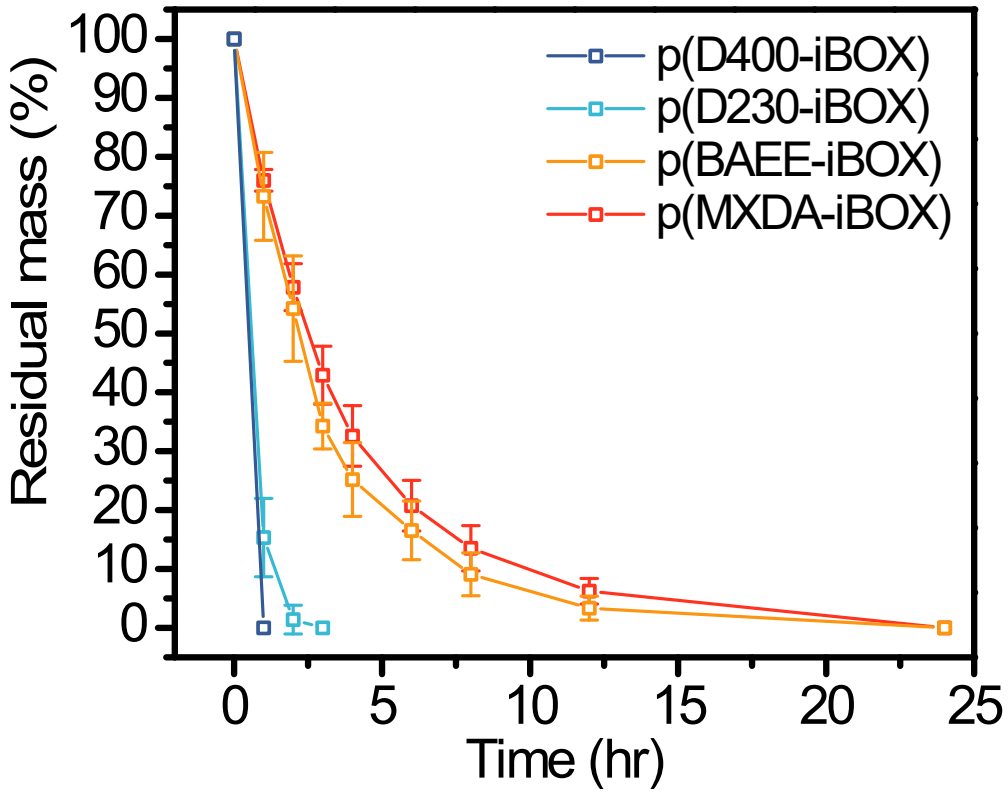

Figure S41. Residual mass vs. time for p(iBOX) networks in 1M HCl/THF (1:1 v/v) at 50 °C.